Unique Bond Breaking in Crystalline Phase Change Materials and the Quest for Metavalent Bonding

Min Zhu, Oana Cojocaru-Mirédin, Antonio M. Mio, Jens Keutgen, Michael Küpers, Yuan Yu, Ju-Young Cho, Richard Dronskowski, and Matthias Wuttig*

Laser-assisted field evaporation is studied in a large number of compounds, including amorphous and crystalline phase change materials employing atom probe tomography. This study reveals significant differences in field evaporation between amorphous and crystalline phase change materials. High probabilities for multiple events with more than a single ion detected per laser pulse are only found for crystalline phase change materials. The specifics of this unusual field evaporation are unlike any other mechanism shown previously to lead to high probabilities of multiple events. On the contrary, amorphous phase change materials as well as other covalently bonded compounds and metals possess much lower probabilities for multiple events. Hence, laser-assisted field evaporation in amorphous and crystalline phase change materials reveals striking differences in bond rupture. This is indicative for pronounced differences in bonding. These findings imply that the bonding mechanism in crystalline phase change materials differs substantially from conventional bonding mechanisms such as metallic, ionic, and covalent bonding. Instead, the data reported here confirm a recently developed conjecture, namely that metavalent bonding is a novel bonding mechanism besides those mentioned previously.

Dr. M. Zhu, Dr. O. Cojocaru-Mirédin, Dr. A. M. Mio, J. Keutgen,
Dr. Y. Yu, Dr. J.-Y. Cho, Prof. M. Wuttig
I. Institute of Physics (IA)
RWTH Aachen University
52056 Aachen, Germany
E-mail: wuttig@physik.rwth-aachen.de
M. Küpers, Prof. R. Dronskowski
Institute of Inorganic Chemistry
RWTH Aachen University
52056 Aachen, Germany
Prof. R. Dronskowski, Prof. M. Wuttig
Jülich-Aachen Research Alliance (JARA-HPC)
RWTH Aachen University
52056 Aachen, Germany
Prof. M. Wuttig
JARA-FIT Institute Green-IT
RWTH Aachen University and Forschungszentrum Jülich
52056 Aachen, Germany

The ORCID identification number(s) for the author(s) of this article can be found under https://doi.org/10.1002/adma.201706735.

Phase change materials (PCMs) have recently attracted significant interest due to their remarkable properties. PCMs can be rapidly and reversibly switched between the amorphous and the crystalline state, yet this transition is accompanied by a pronounced change of optical and electronic properties. This portfolio of properties is very appealing for memory applications and photonics. Indeed, PCMs have been successfully employed in rewriteable optical data storage[1] and have lately also been introduced as fast, yet nonvolatile electronic memories.[2] Their pronounced optical contrast is also utilized in nanophotonic applications[3] and has been discussed as a means to realize ultrafast optical switches.[4]

The compounds identified as PCMs usually either contain chalcogenides such as Te (tellurium) and/or Se (selenium) or pnictogens such as Sb (antimony), where compositions such as $Ge_2Sb_2Te_5$ (GST), $GeSb_2Te_4$, and GeTe are considered as prototypical PCMs. These materials are characterized by an octahedral-like atomic arrangement in the crystalline phase, which has been attributed to bonding via p-electrons, dominating the vicinity of the Fermi energy.[5–7] This distinguishes PCMs from many semiconductors such as Si or GaAs, which are governed by sp^3-hybridization as mirrored by the tetrahedral atomic arrangement and the resulting electronic band structure. To tailor PCMs for a specific application, substantial activities have focused on material optimization, often employing trial and error schemes.[8,9] At the same time, scientists have tried to unravel the origin of the optical contrast between the amorphous and the crystalline phase, which is neither encountered for metallic solids nor ordinary covalent semiconductors such as Si or GaAs. A recent paper has attributed the unusual property portfolio of PCMs to a pronounced change of bonding upon crystallization.[10] While amorphous PCMs utilize ordinary covalent bonding, the special properties found in crystalline PCMs let us believe that there is a new type of bonding in its own right.[11] It is responsible for the unusually high coordination number observed, as well as the extraordinarily large optical dielectric constant, the almost metal-like conductivity, as well as the huge mode specific Grüneisen parameter for transverse optical phonons.[11] We reiterate the three fundamental bonding mechanisms, namely, ionic (with charge transfer), covalent (with shared electrons), and metallic bonding (an extreme form of covalency with too few electrons but too many atoms). In addition, there are dispersive interactions (e.g., van der Waals) and

ADVANCED
SCIENCE NEWS
www.advancedsciencenews.com

ADVANCED
MATERIALS
www.advmat.de

H-bonding, the latter being not a bonding type of its own right but a complicated mélange of the others; because of its omnipresence, it is often considered bonding type no. 5, nonetheless. Hence, we are looking for experimental evidence whether or not the bonding in PCMs can be correlated to the fundamental types of bonding mentioned above. In the present paper we therefore compare the breaking of bonds in different solids as analyzed by laser-assisted field evaporation.[12–14] This study reveals unexpected and pronounced differences in evaporation behavior comparing crystalline with amorphous PCMs as well as ordinary covalent semiconductors. As will be made clear in the following, the bonding in PCMs differs significantly and fundamentally from ordinary covalent semiconductors and metals, so we tentatively suggest a new and unique bonding mechanism.

To compare the laser-assisted field evaporation behavior of different materials, we employ atom probe tomography (APT).[12–14] A schematic illustration of the principle of the APT technique is given in **Figure 1**. A DC voltage of 3–8.0 kV is applied to a needle-shaped specimen with an apex radius of less than 50 nm. Upon laser-assisted field evaporation,[15] atoms found at surface of the needle-shaped sample are ionized and subsequently projected onto a position-sensitive detector. The x- and y- coordinates of the ions registered by the detector, as well as the calculated z-coordinate are used to reconstruct the 3D map.[16] Moreover, these ions can be chemically identified based on time-of-flight mass spectrometry.[17] The final reconstructed 3D maps obtained after performing APT investigations on amorphous GST are shown in **Figure 2**a.

To ensure that no laser-induced crystallization phenomenon takes place during the APT experiments, correlative APT-HRTEM investigations (HRTEM stands for high-resolution transmission electron microscopy) have been performed on various amorphous PCMs before and after exposure of the APT sample to the UV laser pulses. Figure S1 of the Supporting Information shows as an example the high-resolution TEM images and the corresponding fast Fourier transform (FFT) patterns performed on a GST APT sample before being subjected to the UV laser pulses. This first experiment confirms the amorphous structure of the GST specimen. It is worthwhile to note here that neither the Ga beam in focused ion beam (FIB) used to prepare the GST

needle-shaped samples nor the electron beam in TEM affected the amorphous structure of GST. This is mainly due to the careful selection of the experimental conditions (low acceleration voltages for the final cleaning procedure in FIB ≈2–5 keV and low current density in TEM ≈4 nA μm^{-2}). However, after subjecting the GST needle-shaped sample to UV laser pulses of ≈20 pJ, clear fringes belonging to rock-salt phase are observed in the FFT patterns extracted from the top part and right-side of the needle-shaped sample; regions exposed to the focused laser beam (≈2.5 μm beam diameter) as schematically depicted in Figure 2. Hence, the exposure of a GST needle-shaped sample to a laser beam induces the formation of nanoscale crystalline grains.

However, all other amorphous materials studied in this work show no laser-induced crystallization phenomenon. This is clearly shown in Figure S2 of the Supporting Information for the amorphous $GeSe_{0.25}Te_{0.75}$ sample studied by correlative high-resolution APT-TEM experiments. Hence, we can study the laser-assisted bonding breaking for these amorphous materials and compare them with their crystalline counterparts.

To facilitate a comparison of the samples measured, only data obtained under the similar experimental conditions, i.e., 10–20 pJ laser energy, 40–50 K base temperature, 200 kHz laser pulse repetition rate and 1% detection rate are reported here. However, all these experimental conditions had been carefully varied from on material to another (see Figure S3, Supporting Information) to obtain reliable material composition and to avoid artifacts (preferential field evaporation or retention[18]) during APT investigations. Moreover, we mention here that the detection rate characterizes the average percentage of successful pulses, for which ions are field evaporated, contrary to "nulls" where no ions are field evaporated. It needs to be kept generally low and constant during the APT experiments so that no ions are evaporated between subsequent pulses.[19]

We start by comparing two different crystalline samples, a prototypical PCM, i.e., GeTe, with InSb, an ordinary semiconductor utilizing polar covalent bonding. Both materials are narrow band semiconductors, where InSb even has the slightly smaller gap (0.5[20] vs 0.23 eV,[21] respectively). This is in line with InSb being the less ionic phase due to its Pauling
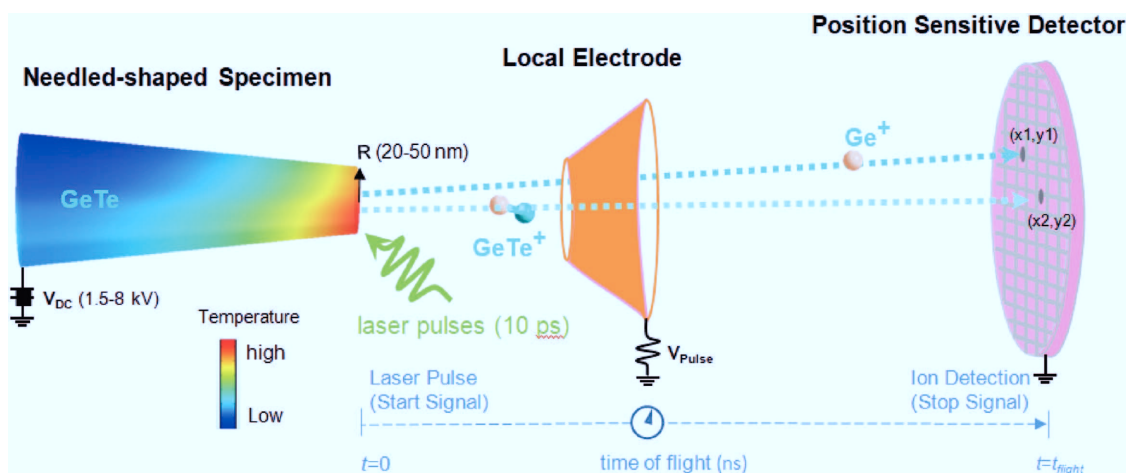

Figure 1. Schematic of the laser-assisted atom probe tomography. The needle-shaped specimen is subjected to a voltage of 3–8 kV and illuminated by 10 ps laser pulses, triggering the field evaporation of atoms or molecular fragments. These atoms or molecular fragments are ionized and successively projected on the position sensitive detector.
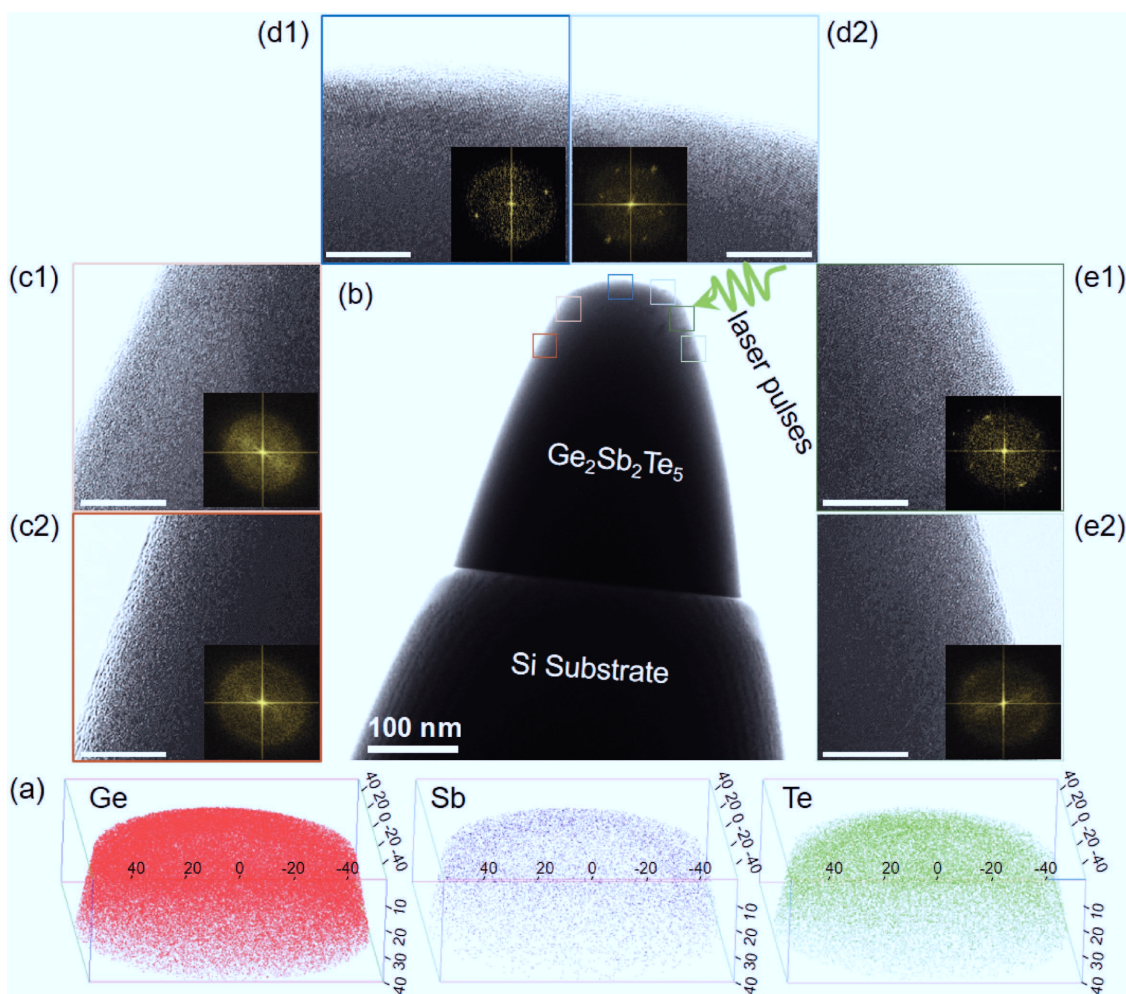
Figure 2. High-resolution correlative APT-TEM investigations showing partial laser-pulse induced crystallization of an amorphous $Ge_2Sb_2Te_5$ tip. a) Reconstructed 3D maps of Ge (red), Sb (blue), and Te (green) atoms obtained from APT. In total, two million ions are field evaporated from the tip by applying laser pulses. b) Bright field TEM image of the resulting tip after the APT experiment. c) Bright field high-resolution TEM images from the left-side of the tip, which show the amorphous state of GST. d,e) Bright field high-resolution TEM images from the top and right-side of the tip, respectively, which clearly show the presence of nanoscale grains in GST. The scale bar corresponds to 10 nm. The insets are the corresponding fast Fourier transformation patterns, showing these grains possess a rock-salt structure. The regions where these nanocrystallites are observed correspond exactly to those regions where the focused laser spot (beam spot size 2.5 µm) hits the specimen.

electronegativity difference (0.1), which is slightly smaller than in the case of GeTe (0.3). Hence, if both materials would be governed by ordinary covalent bonding, we would expect a very similar bond breaking. Surprisingly, however, the laser-assisted evaporation behavior of these two samples differs considerably.

For InSb, for each successful laser pulse, we mostly observe a single ion (90.7% probability) and only in very rare cases more than one ion (called multiple events) is dislodged (**Figure 3**a). More specifically, among the multiple events of InSb, the most popular ones are the twofold events, where two ions are ejected by one laser pulse. The probability of such events is 5.4% as shown in Figure 3b. The fraction of the three- and fourfold event drops sharply to below 1% for both. Other multiple events are rarely found. A strikingly different scenario is observed for a crystalline GeTe specimen, where only 32.1% of the ions are field evaporated as single events while multiple events are abundant. In others word, there is some "collectiveness" at play

when GeTe is disintegrated, not seen for the non-PCM InSb. This immediately raises the question; which mechanism is responsible for the pronounced difference in laser-assisted field evaporation? Before analyzing the bonding mechanism, let us perform similar studies for a related material, i.e., a solid which is also characterized by bonding via p-electrons, but without the characteristic fingerprint of crystalline PCMs. Such a material is GeSe, which also features a distorted octahedral arrangement frequently observed in p-bonded semiconductors. Yet, it has a much lower optical dielectric constant than GeTe. Its coordination number is close to 3, compatible with ordinary covalent bonding following the 8-N rule,[22,23] since the difference of the first nearest neighbor spacing and the next nearest neighbor spacing is considerably larger than in GeTe. For GeSe, the proportion of multiple events drops drastically to 13.3% (see **Table 1**). GeSe has an orthorhombic phase, which does not possess PCM properties, i.e., lacks the pronounced contrast of
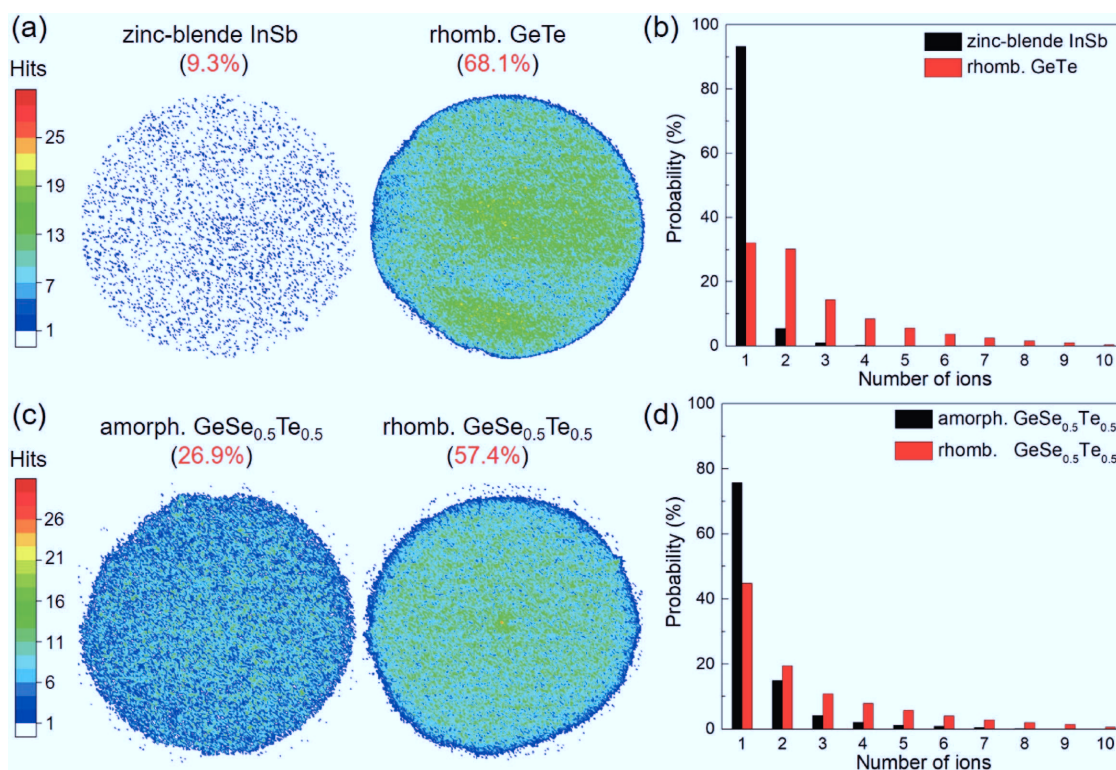
ADVANCED
SCIENCE NEWS
www.advancedsciencenews.com

ADVANCED
MATERIALS
www.advmat.de

Figure 3. Spatial distribution of multiple events on the APT detector for a) zinc-blende InSb, b) rhombohedral (rhomb.) GeTe, c) amorphous (amorph.), and d) rhombohedral $GeSe_{0.5}Te_{0.5}$. Ions in rhombohedral GeTe and crystalline $GeSe_{0.5}Te_{0.5}$ are preferentially evaporated with other ions, resulting in >57.4% proportion of multiple events. By contrast, ions in zinc-blende InSb and amorphous $GeSe_{0.5}Te_{0.5}$ are favorably field evaporated one by one per laser pulse, called single event, and just <26.9% of total ions are detected as multiple events. A total of four million ions are detected for zinc-blende InSb and rhombohedral GeTe, while eight million ions were analyzed for amorphous and crystalline $GeSe_{0.5}Te_{0.5}$. (b,d) The probabilities of one to ten events for the corresponding samples.

optical properties between the amorphous and the crystalline state.[24] This is indicative for a close correlation between the characteristics of the bonding mechanism in crystalline PCMs and the behavior shown upon laser-assisted field evaporation. GeTe, the compound which shows the characteristic fingerprint of crystalline PCMs (pronounced increase of optical dielectric constant, large Born effective charge, high effective coordination number), is characterized by a high probability of multiple events (Figure 3b). On the contrary, the isoelectronic compound GeSe, which utilizes ordinary covalent bonding (as evidenced by the absence of the characteristic features listed before), shows a low probability of multiple events, typically observed for covalently bonded semiconductors. To verify if the change of bonding mechanism is responsible for the change in the field evaporation, the tie line from GeTe to GeSe can be explored. We have studied three compounds along the GeTe–GeSe pseudobinary line, namely, $GeSe_{0.25}Te_{0.75}$, $GeSe_{0.5}Te_{0.5}$, and $GeSe_{0.75}Te_{0.25}$. All three alloys possess a metastable GeTe-like rhombohedral structure where a fraction of the Te sites are randomly occupied by Se atoms[22] and reveal the characteristic fingerprints of crystalline PCMs. As shown in Table 1, 61.7% of the ions in the rhombohedral $GeSe_{0.25}Te_{0.75}$ phase are evaporated as multiple events, just 6.4% lower than that for rhombohedral GeTe. Similarly, rhombohedral $GeSe_{0.5}Te_{0.5}$ and $GeSe_{0.75}Te_{0.25}$ show a high probability of multiple events of more than 57.4%. Interestingly, the rhombohedral phase of

$GeSe_{0.75}Te_{0.25}$ transforms to a more stable hexagonal structure including Ge—Ge bonds upon prolonged annealing.[22] This phase of $GeSe_{0.75}Te_{0.25}$ does not show a pronounced optical contrast upon crystallization, in contrast to typical PCMs.[22,23] This phase has a much lower multiple probability of 36.3%, compared with the rhombohedral phase with the same stoichiometry, which shows the characteristic features of PCMs (67.1%). Hence, these experiments clearly show that the change of bonding mechanism observed along the pseudobinary line between GeTe and GeSe is accompanied by a striking change in the probability of multiple events in laser-assisted field evaporation. This can be seen clearly in **Figure 4**, where the crystalline p-bonded materials (squares) fall in two distinctively different regions. P-bonded crystals, which show the characteristic properties of crystalline PCMs, such as high values of the Born effective charge and significant increases of the optical dielectric constant ε_∞, upon crystallization (green squares) are found in the upper right corner.[24] For all of these materials high probabilities for multiple events are observed. On the other hand, p-bonded materials, like GeSe or hexagonal $GeSe_{0.75}Te_{0.25}$, with small optical dielectric constants characteristic for ordinary covalent semiconductors show low probabilities for multiple events (red squares). From all crystalline phases studied, only those materials with a pronounced change of optical and electronic properties upon crystallization (green squares) are characterized by high values of multiple probability.

**ADVANCED
SCIENCE NEWS**

www.advancedsciencenews.com

**ADVANCED
MATERIALS**

www.advmat.de

Table 1. Probabilities of single event and multiple events in the atom probe tomography (APT) measurements for crystalline and amorphous phase change materials (PCMs), as well as metals and metallic glasses. Since only PCMs exhibit a drastic increase of the optical dielectric constant on crystallization,[8] this increase is used here to distinguish PCMs from non-PCMs. Hence, for each crystalline phase, which reveals a much larger optical constant than its amorphous counterpart, we denote the material as a PCM in the table. Interesting enough, the table shows a clear correlation between the probability for multiple events and the characteristic features of crystalline PCMs, such as high values of the optical dielectric constant ε_∞. This implies that crystalline PCMs utilize a special bonding mechanism, which differs from amorphous PCMs and metals.

Type	Samples	Optical dielectric constant ε_∞	Probability [%]	
			Multiple events	Single event
PCM	Rhombohedral GeTe	34.0	68.1	31.4
	Rhombohedral $GeSe_{0.25}Te_{0.75}$	32.2	61.7	38.0
	Rhombohedral $GeSe_{0.5}Te_{0.5}$	26.3	57.4	42.3
	Rhombohedral $GeSe_{0.75}Te_{0.25}$	24.5	67.1	32.7
	Rock-salt $Ge_2Sb_2Te_5$	33.3	56.2	43.3
Non-PCM	Zinc-blende InSb	16.0	9.30	90.1
	Hexagonal $GeSe_{0.75}Te_{0.25}$	15.9	36.3	63.2
	Orthorhombic GeSe	13.5	13.3	85.6
	Amorphous $GeSe_{0.25}Te_{0.75}$	13.3	29.5	70.2
	Amorphous $GeSe_{0.75}Te_{0.25}$	10.9	21.5	78.1
	Amorphous 11 at% N-doped $Ge_2Sb_2Te_5$	16.0	22.1	77.5
	Cubic Al	≈5	8.0	91.8
	Cubic Fe	≈15[a]	12.6	87.1
	Cubic W	≈19[a]	4.0	95.8
	Amorphous $Cu_{47}Ti_{34}Zr_{11}Ni_8$	—[a]	11.1	87.5

[a]The optical dielectric constant of metals is not well-defined for metals and metallic glasses. It can be derived from the observed plasma frequency and atomic density.

Nevertheless, this conclusion does not yet answer the question if the laser-assisted field evaporation differs between amorphous and crystalline PCMs. A number of amorphous PCMs have hence been studied by APT measurements, as shown in Figure 4, too. Interestingly, amorphous $GeSe_{0.25}Te_{0.75}$ shows only 29.5% probability for multiple events, which further decreases to 26.9% for amorphous $GeSe_{0.5}Te_{0.5}$. The total multiple probability of amorphous $GeSe_{0.5}Te_{0.5}$ is more than two times lower than that of its crystalline counterparts (57.4%), as shown in Figure 3d. For all amorphous PCMs studied we find that the probability of evaporating several ions per laser pulse is significantly lower than the same probability observed for their crystalline counterparts utilizing metavalent bonding. Such an effect is neither observed when comparing amorphous and crystalline GeSe (covalently p-bonded) as well as amorphous and crystalline Si (sp^3-bonded). Hence, as clearly visible in Figure 4, only those solids which possess the characteristic features of crystalline PCMs show high probabilities for multiple events. This conclusion is further corroborated by similar APT investigations for a large variety of PCMs, including SnTe and Sb (Bi)-Te-based alloys, and covalent bonded materials such as Ge. This even holds for the prototypical PCM GST. Amorphous GST, stabilized against crystallization in the APT by doping it with 11 at% nitrogen, showed a low probability for multiple events of 22.1%. If, however, undoped GST was analyzed in the APT, the needle-shaped sample crystallized upon exposure to the short laser pulses leading to the characteristic rock-salt structure in TEM, as shown in Figure 2. For these crystallized samples a drastically increased probability for multiple events of about 56.2% as observed. These APT results are summarized in Figure 4.

Interestingly enough, metals, such as Al, Fe, and W,[25] also always show an extremely low probability of multiple events in APT (≈8%, ≈12.6%, and ≈4%, respectively). Similarly, the amorphous metals, so-called metallic glasses, also present a low value of multiple probability, e.g., 11.1% for $Cu_{47}Ti_{34}Zr_{11}Ni_8$ alloy. These results clearly manifest that materials featuring metallic bonding exhibit an evaporation behavior distinctly different from crystalline PCMs.

The data displayed confirm the conclusion presented above: high probabilities for multiple events are only observed for those material phases, which feature the characteristic properties of crystalline PCMs. Since laser-assisted field evaporation as explored by APT depends on the bonding mechanism in the material studied, our finding implies that crystalline PCMs employ a distinctive bonding mechanism, which differs significantly from ordinary covalent and metallic bonding.

Next, we are trying to understand why a novel bonding mechanism with unique characteristics could be responsible for the high probability for multiple events observed. To do so, the observed evaporation mechanism is analyzed in more detail. Multiple events on the detector are usually attributed to two different mechanisms: field dissociation of molecular ions,[26,27] i.e., the decomposition of a heavier molecular ion into two or more that two smaller ions, or correlated field evaporation,[28] the subsequent evaporation of nearest neighbors after field evaporation of one atom sitting at the surface of the APT sample. The former mechanism typically takes place in nitrides, such as the nanocomposite $TiN-Si_3N_4$[29] where a

**ADVANCED
SCIENCE NEWS**
www.advancedsciencenews.com

**ADVANCED
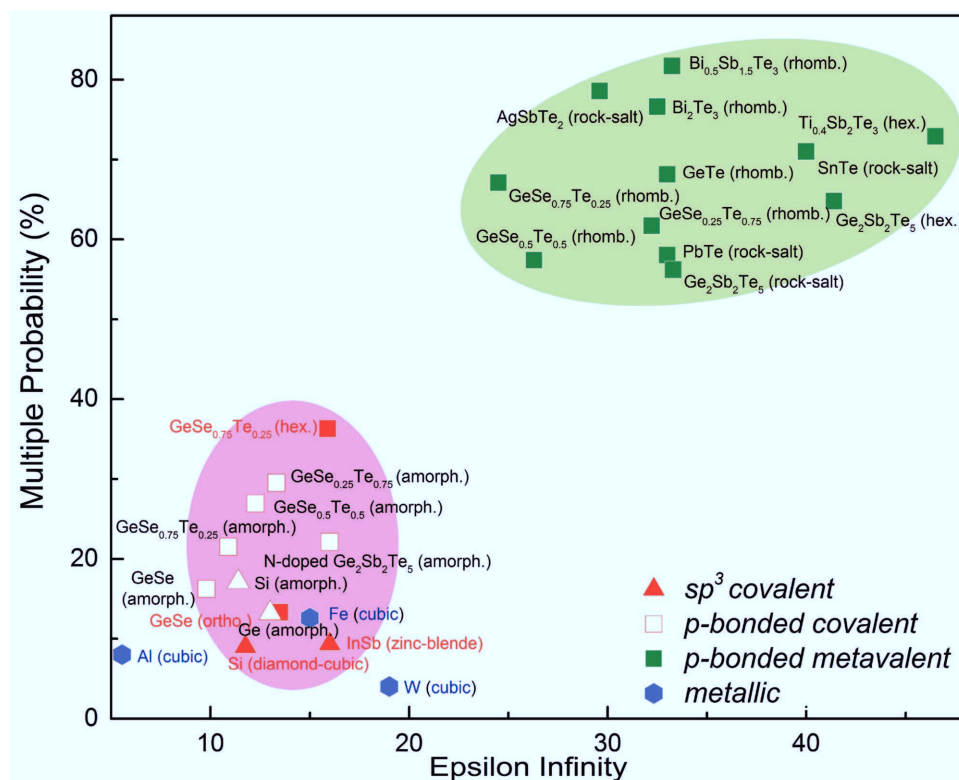MATERIALS**
www.advmat.de

Figure 4. Correlation between multiple probability and bonding mechanism. A wide variety of materials are shown which can be categorized into two classes considering their bonding mechanism. Covalently bonded materials are denoted in red, while compounds utilizing the characteristic features of crystalline PCMs are depicted in green and metals are displayed in blue. Open symbols characterize amorphous phases, filled symbols depict crystalline phases, while triangles describe sp^3-bonded materials (tetrahedral atomic arrangement), squares denote p-bonded compounds (octahedral-like atomic arrangement) and hexagons denote crystalline metals with fcc or bcc structure. amorph., rhomb., hex., and ortho. represent amorphous, rhombohedral, hexagonal, and orthorhombic phases, respectively. Crystalline PCMs have much larger values of the optical dielectric constant (ε_∞) than all other materials and can hence be found on the right side of the viewgraph. Interestingly, these materials also differ from all other materials in terms of laser-assisted field evaporation. Crystalline PCMs are characterized by a high number of multiple events, not observed in any other material class studied here. This provides strong evidence for a different bonding mechanism in crystalline PCMs, which is characterized by a higher "collectiveness" in bond rupture.

high proportion of multiple events (≈55%) was detected. The later one is a common, yet not the prevailing process in most of the materials studied by APT, since atoms situated in kink sites are less strongly bonded. Thus, they can easily be evaporated together with their neighbor(s).[30] However, the proportion of multiple events in this case is usually low (not higher than 10–20%).[28,30] Furthermore, there is the particular case of carbon (boron)-doped steel or carbides[31,32] where between 30% and 46% of multiple events have been registered. This high proportion of multiple events is due to unexpected C or B surface migration prior to field evaporation. This is rather a measurement artefact during the APT experiments which leads to an inhomogeneous C or B distribution on the detector.[31–34] On the contrary, the distribution of multiple events on the detector is homogeneous for crystalline PCMs (as can be seen in Figure 3a,c), unlike the case of carbon (boron) doped steel. Hence, we are not dealing with a measurement artifact.

In the following, we will show that none of the two mechanisms discussed above (field dissociation and correlated field evaporation) can account for the high probability for multiple events observed in materials where metavalent bonding prevails. The high fraction of multiple events observed cannot be attributed to field dissociation of molecular ions. This process

leads to dissociation tracks, which we do not observe for most of PCMs (as discussed in detail in Figure S4, Supporting Information). Furthermore, the high probability of multiple events is even preserved when the electric field applied to the needle-shaped sample is decreased, i.e., the laser pulse energy is increased (see Figure S3, Supporting Information). All these findings are incompatible with the mechanism of field dissociation of molecular ions. Finally, the extraordinary high multiple probability observed for crystalline PCMs cannot also be explained by conventional correlated field evaporation.[28] For such materials, the probability for multiple events is much higher than 10–20%. Therefore, such high fraction of multiple events can not only come from such kink sites. Hence, the high level of "collectiveness" observed in the enhanced correlated field evaporation mechanism is an intrinsic property of crystalline PCMs.

In the following we will try to characterize this bonding mechanism further and relate it to the features observed in the field-evaporated dissociation studied by APT. The bonding mechanism encountered in crystalline PCMs is characterized by a unique property portfolio.[11] These properties include the following characteristics: an atomic arrangement incompatible with the 8-N rule, a moderate electronic conductivity, high
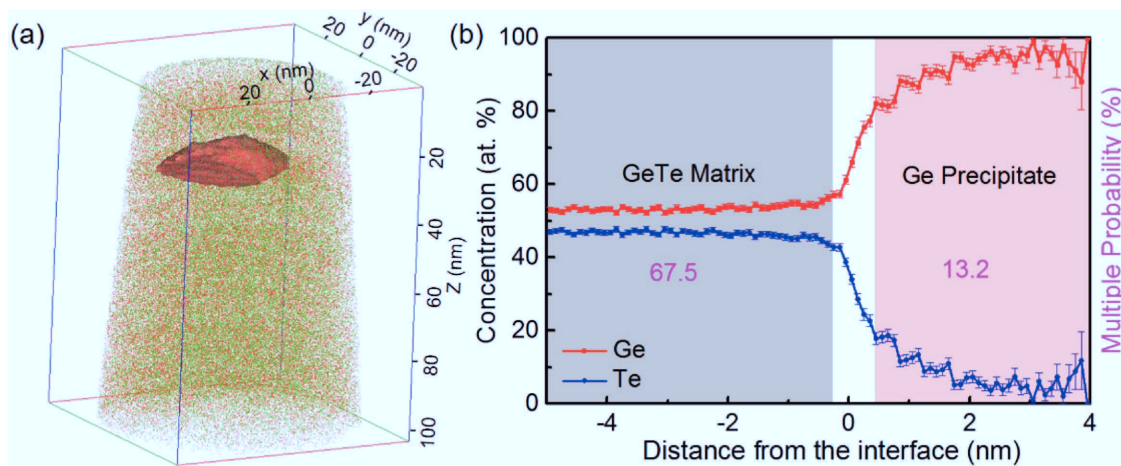
**ADVANCED
SCIENCE NEWS**
_____
www.advancedsciencenews.com

**ADVANCED
MATERIALS**
www.advmat.de

Figure 5. Characterization of a crystalline GeTe sample by APT. a) 3D reconstruction maps of a rhombohedral Ge-rich GeTe film obtained from APT. Red and green dots represent Ge and Te atoms, respectively. The red area represents the 60.9 at% Ge iso-concentration surface, implying the appearance of a Ge precipitate. b) Proximity histogram concentration profiles of Ge and Te for the Ge precipitate. The stoichiometry of the sample, $Ge_{53.5}Te_{46.5}$, slightly deviates from stoichiometric $Ge_{50}Te_{50}$, which is causing phase segregation. Noticeably, the multiple probability undergoes a steep drop from 67.5% for the matrix, which shows that metavalent bonding prevails there, to 13.2% for the Ge precipitate. Hence, ordinary covalent bonding characterizes the precipitate. This example shows that crystallization of PCMs and formation of metavalent bonds can be detected by APT on the nanoscale.

values of the optical dielectric constant, as well as large Born effective charges and a pronounced Grüneisen parameter for transverse optical phonons. The underlying bonding mechanism is to be located between metallic and covalent bonding, thus the electrons are neither fully localized as in covalent bonding, nor fully delocalized as in metallic bonding.[11] That is to say that the bonding orbitals also mix with the atomic environment beyond the nearest neighbors but not as far as in metallic materials. Even upon breaking an individual bond, the second-nearest neighbor bonding interactions are strong enough such that multiple events are observed. In the amorphous state, however, the electrons are localized between two adjacent atoms, hence producing few multiple events. In this bonding mechanism, the atomic arrangement is in line with the 8-N rule, the electronic conductivity is drastically lower, the optical dielectric constant ε_∞ is considerably smaller and the same holds for the Born effective charge Z^*. This combination of properties is characteristic for ordinary covalent bonding. Therefore, the field evaporation mechanism responsible for the extraordinary high probability of multiple events is closely related to the exceptional properties of the bonding mechanism observed here. Since the bonding mechanism differs substantially from the bonding mechanisms discussed in textbooks of material science and solid state physics, i.e., ionic, covalent, metallic, H- and van der Waals bonding, it deserves a genuine name. We have recently suggested the term "metavalent bonding" for this mechanism, since it is closely related to metallic and covalent bonding, yet clearly goes beyond ordinary covalent bonding, as described by the Greek word _meta_ ($\mu\varepsilon\tau\alpha$).[11]

Traditionally, APT is utilized to investigate the atomic distribution and composition in three-dimensions on a subnanometer scale.[17] Thanks to its outstanding capabilities, APT can be applied to study nanoscale phase separation (or phase stability) and atomic diffusion in the vicinity of the defects in PCMs or devices.[35,36] Now, we can combine these features with

the ability of the APT to detect nanoscale regions distinguishing between metavalent and ordinary bonding as demonstrated in **Figure 5**, where a ≈30 nm size Ge-rich precipitate is observed in the crystalline GeTe matrix. Such Ge precipitates are easily formed, if the GeTe matrix contains an excess of Ge, in this case a Ge concentration of 53.5 at%.[37] The APT does not only verify the formation of the Ge precipitate, but also reveals a sudden drop for the probability of multiple events, from 67.5% for the GeTe matrix, to 13.2% for the Ge precipitate. This implies that the bonding changes from metavalent for the GeTe matrix, which hence is crystalline, to the Ge precipitate, which does not show metavalent bonding, but is apparently covalently bonded. This kind of information is vital to doping-engineered PCMs, often possessing nanoscale phase segregation.[38,39]

In summary, we have utilized APT for a systematic investigation of differences in laser-assisted field evaporation in a large number of compounds, including amorphous and crystalline PCMs. Our study reveals significant differences in field evaporation, where a high probability of multiple events has been found for crystalline PCMs exclusively. The specifics of this field evaporation are unlike any other material class. These findings provide strong experimental evidence that the bonding mechanism in crystalline PCMs differs substantially from conventional bonding mechanisms such as metallic, ionic, and covalent bonding. Instead, the data reported here confirm a recently developed conjecture, namely that metavalent bonding is a novel bonding mechanism.[11] This insight can be utilized in different ways, it can be employed to investigate and compare bonding mechanisms in several phases of the same stoichiometry (such as the two $GeSe_{0.75}Te_{0.25}$ phases studied here). APT investigations can also be used to identify new compounds, which employ metavalent bonding. This has already been implicitly demonstrated in Figure 4, where Bi_2Te_3 is identified as a material which possesses metavalent bonding, too. This finding can be attributed to significant coupling across the van der Waals-like gaps in rhombohedral V_2VI_3 phases.[40] The

**ADVANCED
SCIENCE NEWS**
www.advancedsciencenews.com

**ADVANCED
MATERIALS**
www.advmat.de

conclusions derived here also show unambiguously that PCMs utilized for rewriteable optical and novel electronic memories are actually bond change materials, where the bonding changes upon crystallization from covalent bonding to metavalent bonding. We are not aware of any other application where a change of bonding mechanism is utilized without a change in composition. These findings also open a novel approach toward nanoscale analysis of the bonding mechanism in PCMs and material optimization via doping. This opportunity is crucial for optimization of PCMs in applications ranging from neuromorphic computing to nonvolatile electronic memories.

Experimental Section

Sample Preparation: Most crystalline samples were synthesized from the elements in a vacuum-sealed quartz ampoule.[22] The amorphous samples were deposited on Si substrates by sputtering employing alloy target of 99.99% purity. Annealing these amorphous specimens enabled the preparation of crystalline samples, too. The stoichiometry of the resulting samples was obtained from energy dispersive spectroscopy. Optical dielectric constants were extracted from Fourier transform infrared spectroscopy.[10]

Needle-Shaped Sample Preparation: The APT needle-shaped samples were prepared by standard lift-out procedure, using a dual-beam focus ion beam (FEI Helios Nanolab 650). These samples, with a top radius smaller than 100 nm, were mounted on flat top Si microtips.

APT Measurement: Subsequently, these APT needle-shaped samples were put into a $\approx 10^{-11}$ mbar high vacuum, and then measured using a local electrode atom probe (LEAP 4000 X Si, Cameca Instruments) in laser pulse mode at a base temperature of 50 K. Laser pulses of 355 nm wavelength, 200 kHz frequency, 10–20 ps pulse duration were applied. The obtained data were analyzed by the software IVAS 3.6.12. A more detailed analysis of multiple events was performed using the in-house developed software called EPOSA, which allows the multiple events to be reconstructed in 3D.

APT-TEM Correlation Experiments: For this study, two amorphous GST APT samples were mounted on half-cut molybdenum TEM grid. One of them was measured by APT and the APT run was stopped after obtaining two million ions. The other APT sample, called the reference sample, was not measured. Subsequently, these two APT samples were further analyzed by FEI Tecnai F20 TEM in bright field mode. While APT is ideally suited to study the elemental distribution on the sub-nanometer scale, APT faces a potential problem when studying PCMs. These materials are well-known for their rapid crystallization upon exposure to short laser pulses. This process occurs very rapidly at rather low crystallization temperatures (between 423 and 453 K for the most known PCMs such as GST and GeTe).

It is mandatory to verify that APT measurements can be performed on amorphous samples without being crystallized by the picosecond laser pulses applied in APT. The formation of crystalline grains is possible, since the peak temperature of the needle-shaped sample subjected to laser-pulses is much higher than the applied base temperature between 20 and 50 K. For example, the peak temperature measured on W specimens subjected to a 515 nm laser with 0.5 µJ reached maximum temperatures of 300 K[18,41,42] under standard experimental conditions. To determine the peak temperature of a highly conductive needle-shaped sample, the dependence of the voltage on temperature for voltage pulsed mode or on laser energy for laser-pulsed mode need to be measured at fixed detection rate, pulse repetition rate, and fixed samples-detector distances, as explained by Marquis and Gault.[43] Unfortunately, the determination of peak temperature for the amorphous GST sample with poor conductivity was impossible due to immediate fracture under high voltage pulses. However, the existence of diffraction spots on the FFT pattern imply that the peak temperature reaches the T_c of traditional GeTe-Sb$_2$Te$_3$ PCMs (373–453 K)[43] even when the experiments were performed at a very low base temperature of about 20 K.

Supporting Information

Supporting Information is available from the Wiley Online Library or from the author.

Conflict of Interest

The authors declare no conflict of interest.

[1] M. Wuttig, N. Yamada, *Nat. Mater.* **2007**, *6*, 824.
[2] A. Pirovano, A. L. Lacaita, A. Benvenuti, F. Pellizer, R. Bez, *IEEE Trans. Electron Devices* **2003**, *51*, 452.
[3] M. Wuttig, H. Bhaskaran, T. Taubner, *Nat. Photonics* **2017**, *11*, 465.
[4] L. Waldecker, T. A. Miller, M. Rude, R. Bertoni, J. Osmond, V. Pruneri, R. E. Simpson, R. Ernstorfer, S. Wall, *Nat. Mater.* **2015**, *14*, 991.
[5] N. Yamada, T. Matsunaga, *J. Appl. Phys.* **2000**, *88*, 7020.
[6] M. Luo, M. Wuttig, *Adv. Mater.* **2004**, *16*, 439.
[7] D. Lencer, M. Salinga, M. Wuttig, *Adv. Mater.* **2011**, *23*, 2030.
[8] S. Raoux, R. M. Shelby, J. J. Sweet, B. Munoz, M. Salinga, Y.-C. Chen, Y.-H. Shih, E.-K. Lai, M.-H. Lee, *Micro. Eng.* **2008**, *85*, 2330.
[9] S. Kim, P. Y. Du, J. Li, M. Breitwisch, Y. Zhu, S. Mittal, R. Cheek, T.-H. Hsu, M. H. Lee, A. Schrott, S. Raoux, H. Y. Cheng, S.-C. Lai, J. Y. Wu, T. Y. Wang, E. A. Joseph, E. K. Lai, A. Ray, H.-L. Lung, C. Lam, *Proc. Tech. Pap. - Int. Symp. VLSI Technol., Syst., Appl. (VLSI-TSA)* **2012**, 1.
[10] K. Shportko, S. Kremers, M. Woda, D. Lencer, J. Robertson, M. Wuttig, *Nat. Mater.* **2007**, *7*, 653.
[11] M. Wuttig, V. L. Deringer, X. Gonze, C. Bichara, J.-Y. Raty, *Mater. Sci.* **2017**, arXiv: 1712.03588.
[12] D. Blavette, A. Bostel, J. M. Sarrau, B. Deconihout, A. Menand, *Nature* **1993**, *363*, 432.
[13] T. F. Kelly, M. K. Miller, *Rev. Sci. Instrum.* **2007**, *78*, 031101.
[14] B. Gault, F. Vurpillot, A. Vella, M. Gilbert, A. Menand, D. Blavette, B. Deconihout, *Rev. Sci. Instrum.* **2006**, *77*, 043705.
[15] M. K. Miller, *Atom Probe Tomography: Analysis at the Atomic Level*, Springer Science & Business Media, Berlin, Germany **2012**.

[16] B. Gault, M. P. Moody, J. M. Cairney, S. P. Ringer, *Mater. Today* **2012**, *15*, 378.

[17] B. Gault, M. P. Moody, J. M. Cairney, S. P. Ringer, *Atom Probe Microscopy*, Springer, New York **2012**.

[18] O. Cojocaru-Mirédin, L. Abdellaoui, M. Nagli, S. Zhang, Y. Yu, C. Scheu, D. Raabe, M. Wuttig, Y. Amouyal, *ACS Appl. Mater. Interfaces* **2017**, *9*, 14779.

[19] D. J. Larson, T. J. Prosa, R. M. Ulfig, B. P. Geiser, T. F. Kelly, *Local Electrode Atom Probe Tomography*, Vol. *1*, Springer, New York **2013**.

[20] J. L. F. Da Silva, A. Walsh, H. Lee, *Phys. Rev. B* **2008**, *78*, 224111.

[21] I. Vurgaftman, J. R. Meyer, L. R. Ram-Mohan, *J. Appl. Phys.* **2001**, *89*, 5815.

[22] M. Küpers, P. M. Konze, S. Maintz, S. Steinberg, A. M. Mio, O. Cojocaru-Mirédin, M. Zhu, M. Müller, M. Luysberg, J. Mayer, M. Wuttig, R. Dronskowski, *Angew. Chem., Int. Ed.* **2017**, *56*, 10204.

[23] S. Jakobs, A. von Hoegen, M. Xu, M. Drögeler, C. Stampfer, R. P. S. M. Lobo, A. Piarristeguy, A. Pradel, M. Wuttig, unpublished.

[24] D. Lencer, M. Salinga, B. Grabowski, T. Hickel, J. Neugebauer, M. Wuttig, *Nat. Mater.* **2008**, *7*, 972.

[25] D. Saxey, *Ultramicroscopy* **2011**, *111*, 473.

[26] M. Muller, B. Gault, G. D. Smith, C. R. M. Grovnor, *J. Phys. Conf. Ser.* **2011**, *36*, 012031.

[27] B. Gault, D. W. Saxey, M. W. Ashton, S. B. Sinnott, A. N. Chiaramonti, M. P. Moody, D. K. Schreiber, *New J. Phys.* **2016**, *18*, 033031.

[28] F. De Geuser, B. Gault, A. Bostel, F. Vurpillot, *Surf. Sci.* **2007**, *601*, 536.

[29] F. Tang, B. Gault, S. P. Ringer, J. M. Cairney, *Ultramicroscopy* **2010**, *110*, 836.

[30] K. M. Bowkett, D. A. Smith, in *Defects in Crystalline Solids, Field Ion Microscopy*, Vol. *2* (Eds: S. Amelinckx, R. Gevers, J. Nihoul), North Holland Publishing Company, The Netherlands **1970**.

[31] L. Yao, B. Gault, J. M. Cairney, S. P. Ringer, *Philos. Mag. Lett.* **2010**, *90*, 121.

[32] M. Thuvander, A. Kvist, L. J. S. Johnson, J. Weidow, H.-O. Andren, *Ultramicroscopy* **2013**, *132*, 81.

[33] B. Gault, F. Danoix, K. Hoummada, D. Mangelinck, H. Leitner, *Ultramicroscopy* **2012**, *113*, 182.

[34] R. Marceau, P. Choi, D. Raabe, *Ultramicroscopy* **2013**, *132*, 239.

[35] K. Thompson, P. L. Flaitz, P. Ronsheim, D. J. Larson, T. F. Kelly, *Science* **2007**, *317*, 1370.

[36] O. Cojocaru-Mirédin, Y. Fu, A. Kostka, R. Sáez-Araoz, A. Beyer, N. Knaub, K. Volz, C.-H. Fischer, D. Raabe, *Prog. Photovoltaics: Res. Appl.* **2015**, *23*, 705.

[37] T. Chattopadhyay, J. Boucherle, *J. Phys. C: Solid State Phys.* **1987**, *20*, 1431.

[38] S. Privitera, E. Rimini, R. Zonca, *Appl. Phys. Lett.* **2004**, *85*, 3044.

[39] S. Raoux, R. M. Shelby, J. Jordan-Sweet, B. Munoz, M. Salinga, Y.-C. Chen, Y.-H. Shih, E.-K. Lai, M.-H. Lee, *Microelectron. Eng.* **2008**, *85*, 2330.

[40] R. Wang, F. R. L. Lange, S. Cecchi, M. Hanke, M. Wuttig, R. Calarco, *Adv. Funct. Mater.* **2018**, 1705901.

[41] A. Cerezo, G. Smith, P. Clifton, *Appl. Phys. Lett.* **2006**, *88*, 154103.

[42] E. A. Marquis, B. Gault, *J. Appl. Phys.* **2008**, *104*, 084914.

[43] N. Yamada, E. Ohno, K. Nishiuchi, N. Akahira, M. Takao, *J. Appl. Phys.* **1991**, *69*, 2849.